Scaling of the Nucleation Rate and a Monte Carlo Discrete Sum Approach to Water Cluster Free Energies of Formation†

B. N. Hale‡ and D. J. DiMattio§

Physics Department, University of Missouri—Rolla, Rolla, Missouri 65409, and Physics Department, St. Bonaventure University, St. Bonaventure, New York 14778

Received: June 1, 2004; In Final Form: September 23, 2004

The intent of this work is to examine small cluster discrete size effects and their effect on the free energy of cluster formation. There is evidence that such terms can cancel in part the temperature dependence of the monomer flux factor of the classical nucleation rate and result in a scaled form for the nucleation rate. In this work, Monte Carlo configurational free energy differences between neighboring sized *n* molecule TIP4P water clusters are calculated and used in a Monte Carlo discrete summation (MCDS) technique to generate steady-state nucleation rates. The free energy differences, when plotted versus $n^{-1/3}$, show evidence of a bulklike effective surface tension for $n \geq 10$, and for the range of *T* examined the free energy differences appear to scale in temperature like $(T_c/T - 1)$. This scaling can provide estimates of nucleation rates for arbitrary temperatures within the range of *T* simulated. Nucleation rates generated from the model TIP4P free energy differences are compared with the experimental water nucleation rate data of Wölk and Strey (*J. Chem. Phys.* **2001**, *105*, 11683) and with the data of Miller et al. (*J. Chem. Phys.* **1983**, *78*, 3204). The TIP4P MCDS results provide some evidence of the cancellation effect and generate the scaling of the nucleation rate data at higher temperatures. The magnitudes of the nucleation rates are, however, too large by a factor of 10^4. Other discrete sum models are also presented and give similar results.

I. Introduction

Over seventy years ago Volmer and Weber,[1] and shortly thereafter others,[2−4] developed a classical steady-state nucleation rate formalism (CNT) that encompassed the basic physical features of the nucleation process.[5,6] This rate, at which embryos of the new phase are formed from a parent phase, plays a major role in many physical phenomena. For many years, the classical nucleation rate, J_{CNT}, has been used with moderate success to describe the onset conditions for nucleation, that value of the supersaturation ratio, S_{cr}, for which the nucleation rate becomes observable at a given temperature, *T*. In the classical model, the energy of formation of the critical cluster, $(16\pi/3)\,[(\sigma/kT)^3/(\rho_{liq}\ln S)^2]$, can be calculated from σ, ρ_{liq}, and $S = P/P_o$, the bulk liquid surface tension, liquid number density, and supersaturation ratio of ambient (equilibrium) vapor pressures, *P* (P_o). Beginning in the 1980s, a number of experimental nucleation rate measurements[7−16] were reported for a range of *T* and *S*, and the classical model was subjected to stringent tests. At the same time, it was pointed out[17−19] that the temperature dependence of vapor-to-liquid nucleation rate data for toluene[8] and nonane[9] appeared to be better described by a scaled energy of formation, $[16\pi\Omega^3(T_c/T - 1)^3/3[\ln S]^2]$, where T_c is the vapor−liquid critical temperature and Ω is the excess surface entropy per molecule divided by the Boltzmann constant, *k*.[17]

This scaled energy of formation is a "corresponding states" form obtained by replacing the surface tension in the classical model with $\sigma = \sigma'_o[T_c - T]$. From the classical model, it follows that $\Omega = \sigma'_o/(k\rho_{liq}^{2/3})$. Experimentally, Ω is found to be a nearly universal constant (approximately 2 for normal liquids and about 1.5 for substances with a dipole moment), and one can estimate nucleation rates for a wide range of substances from a corresponding states approach. The scaled energy of formation depends on the ratio, $\ln S/(T_c/T - 1)^{3/2}$, and for a constant nucleation rate, this ratio implies an approximate scaling law for *S* and *T*. The exponent, 3/2, arises from the dependence on volume and surface area of quantities in the energy of formation. Scaling of the nucleation rate near the critical point was addressed some time ago by Fisher,[20] Binder and Stauffer,[21] and Binder.[22] However, the scaled form near the critical point depends on critical exponents, and (for three-dimensional fluids) one finds the comparable expression, $\ln S/(1 - T/T_c)^{\beta\delta}$ with $\beta\delta = 1.54$ for $\beta = 0.355$ and $\delta = 4.35$.[22] At lower temperatures, rather than $(1 - T/T_c)$, we have used $(T_c/T - 1)$, which seems to follow more naturally from a Boltzmann-like factor and has a larger range of applicability.[17] Near the critical point, where $T/T_c \approx 1$, the forms are nearly indistinguishable.

The more difficult aspect of scaling the nucleation rate at lower temperatures, as discussed in the present paper, has been understanding why the classical model monomer kinetic flux factor temperature dependence appears to be absent in the experimental data. The classical nucleation rate as a function of *T* and *S* is given by[2]

$$J_{CNT} = J_{o,class}\exp\left[\frac{-16\pi}{3}\frac{\left(\frac{\sigma}{kT}\right)^3}{(\rho_{liq}\ln S)^2}\right] \qquad (1)$$

where using *m*, the molecular mass, the monomer flux factor is

* Author to whom correspondence should be addressed. E-mail: bhale@umr.edu.

† Part of the special issue "Frank H. Stillinger Festschrift".

‡ University of Missouri−Rolla.

§ St. Bonaventure University.

10.1021/jp0476343 CCC: $27.50
Published on Web 11/12/2004

$$J_{\text{o,class}} = \left[\frac{P_o}{kT}\right]^2 \left(\frac{2\sigma}{\pi m}\right)^{1/2} \frac{S^2}{\rho_{\text{liq}}} \tag{2}$$

The major temperature dependence in $J_{\text{o,class}}$ has an exponential form

$$\left[\frac{P_o}{kT}\right]^2 \approx {\rho_c}^2 \exp\left[-2 \ln \frac{P_c}{P_o}\right] \approx {\rho_c}^2 \exp\left[-2W_o\left(\frac{T_c}{T} - 1\right)\right] \tag{3}$$

where, for example, $W_o \approx 7.5$ for water. Because the data suggested negligible temperature dependence in $J_{\text{o,class}}$, a simple scaling law, $\ln S_{cr} = 0.53\ \Omega^{3/2}(T_c/T - 1)^{3/2}$, was proposed for onset nucleation conditions.[17] Surprisingly, this scaling law agreed with data for a range of materials far better than would be justified by the form for $J_{\text{o,class}}$.[19,23−26] In fact, the toluene and nonane data over a range of nucleation rates above onset appeared to agree well with a simple scaled model, J_{scaled}[19]

$$J_{\text{scaled}} = J_o \exp\left[-\frac{16\pi\Omega^3\left[\frac{T_c}{T} - 1\right]^3}{3[\ln S]^2}\right] \tag{4}$$

where J_o is a constant well approximated by one event per thermal wavelength cubed per second at T_c. In most cases, one can use $J_o = 10^{26}$ cm^{-3} s^{-1}.

It was not until the mid-1990s that it became generally recognized that the classical nucleation rate model has the wrong temperature dependence.[6,14,16,27,28] That is, the classical model tends to underestimate the experimental nucleation rate at low temperatures and overestimate the rate at high temperatures, often giving agreement at one temperature in the range where the data exist. For most substances, the resulting errors range from 1 to 4 orders of magnitude. The typical discrepancy of J_{CNT} with experiment is shown in Figure 1 for the water nucleation rate data of Wölk and Strey[15] and for the data of Miller et al.[7] In this figure, the experimental nucleation rates at each temperature and supersaturation ratio pair (T_{exp}, S_{exp}) are plotted versus the corresponding classical model nucleation rate predictions, $J_{\text{CNT}}(T_{\text{exp}},S_{\text{exp}})$. If the classical model provided an exact prediction, then all of the points would fall on the dotted line. Instead, data points along lines of approximately constant temperature spread out horizontally from the dotted line, indicating a classical model temperature dependence not observed in the data. The total displacement (about 3 orders of magnitude) is roughly of the form $\exp[-2W_o(T_c/T - 1)]$ for the water data.[29] The actual temperature spread is 218 to 259 K, giving $\delta[2W_oT_c/T] \approx 6.9$, about 3 orders of magnitude. Recently, Wölk et al.[30] published an empirical fitting factor, $\exp[A + B/T]$, with $A = -27.56$ and $B = 6500$ K, for which $J_{\text{CNT}} \exp[A + B/T] = J_{\text{exp}}$ where J_{exp} is the water nucleation rate data of Wölk and Strey[15] plotted in Figure 1. One can also show[31] that this fitting factor for water transforms the classical rate, J_{CNT}, for water into a form nearly identical with the scaled nucleation rate model, J_{scaled}, in eq 4. In the latter expression for J, the predominant temperature dependence is in the scaled energy of formation. A comparison of J_{scaled} with J_{exp} is shown in Figure 2 where the experimental data in Figure 1 is plotted versus $J_{\text{scaled}}(T_{\text{exp}},S_{\text{exp}})$, with $\Omega = 1.45$. The latter value of Ω is in the range of that expected for polar substances, but in general larger than the excess surface entropy per molecule for water as determined from the bulk liquid surface tension. The magnitude of Ω determines the slope but does not alter the temperature dependence in Figure 2.

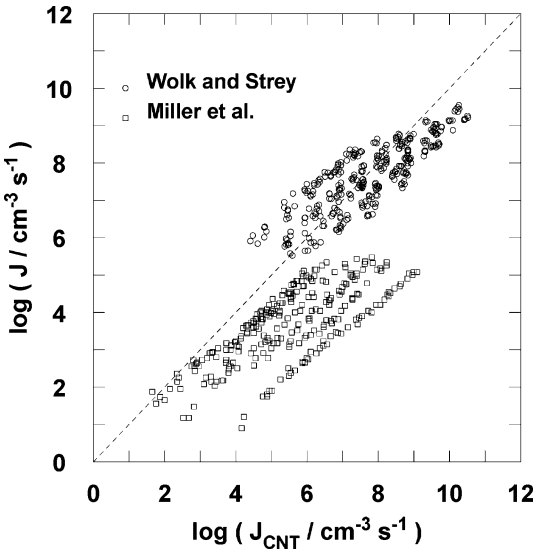

Figure 1. The experimental homogeneous nucleation rate data for water of Wölk and Strey[15] (○) and Miller et al.[7] (□) compared with the classical model prediction. The dashed line indicates perfect agreement.

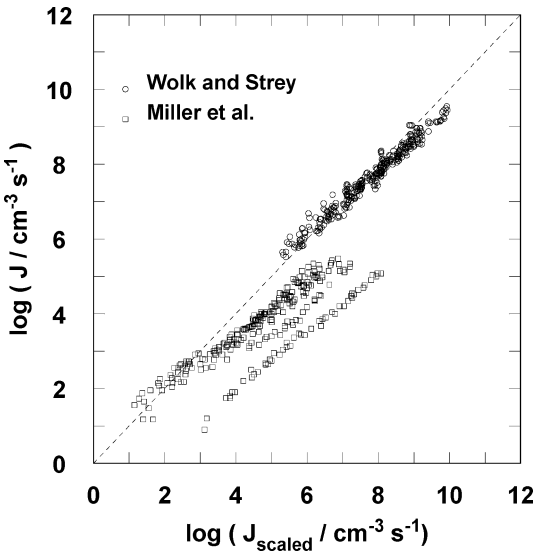

Figure 2. The experimental homogeneous nucleation rate data for water of Wölk and Strey[15] (○) and Miller et al.[7] (□) compared with the scaled model prediction using $\Omega = 1.45$.

Experimentalists have traditionally plotted J_{exp} versus $\ln S$. An application of the scaling that requires no knowledge of Ω is shown in Figure 3 where $\log J_{\text{exp}}$ is plotted versus the scaled supersaturation[17]

$$\ln S_{\text{scaled}} = \frac{\ln S}{\left[\frac{T_c}{T} - 1\right]^{3/2}} \tag{5}$$

To keep the scaled supersaturation in the same range as $\ln S$ in the traditional plot, the scaled supersaturation in Figure 3 is normalized with the factor $(T_c/240 - 1)^{3/2}$. One can see that the lines of data corresponding roughly to constant temperatures that spread out in a standard $\log J_{\text{exp}}$ versus $\ln S$ plot (indicated by the dashed lines of the empirical fitting function) collapse onto a single line (data points indicated with open circles) when $\ln S$ is scaled with $(T_c/T - 1)^{3/2}$. Similar plots demonstrate scaling of the toluene data and, to a lesser degree, the nonane homogeneous nucleation rate data.[32] In this approach, one can

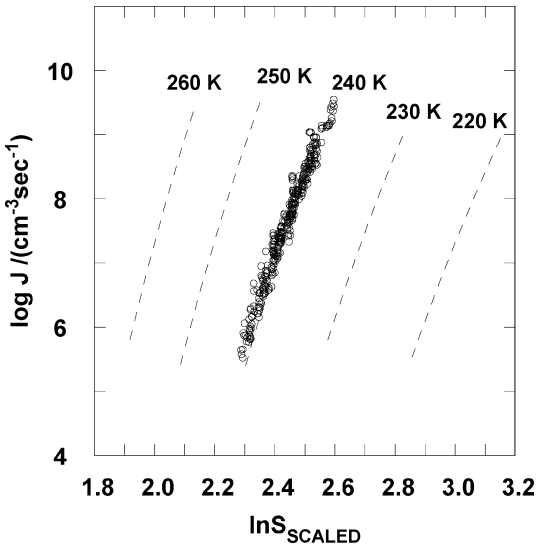

Figure 3. The homogeneous water nucleation rate data of water, Wölk and Strey[15] (○) plotted versus the scaled supersaturation, $\ln S/[T_c/T - 1]^{3/2}$. The scaled supersaturation is multiplied by a normalizing constant, $[T_c/240 - 1]^{3/2}$, so that the values fall in the same range as $\ln S$. The dashed lines (from the empirical fit to the experimental data[15]) indicate where the points fall if $\log J_{exp}$is plotted versus $\ln S$.

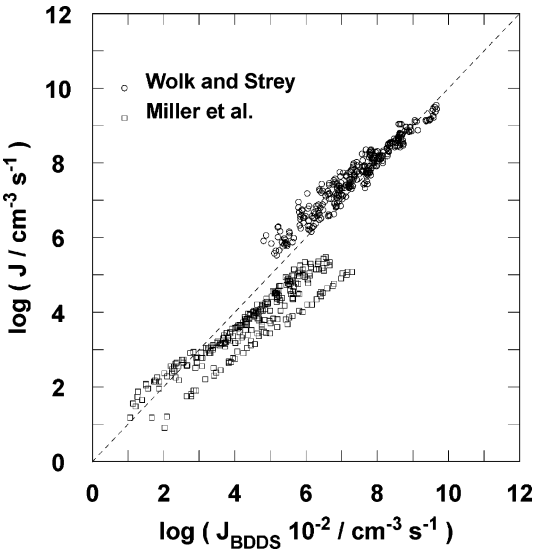

Figure 4. The experimental homogeneous nucleation rate data for water of Wölk and Strey[15] (○) and Miller et al.[7] (□) compared with the discrete sum over small cluster free energy differences, using $\Sigma_{n'=2,3,...n}\delta[An'^{2/3} + \tau \ln n' - n' \ln S]$, $\tau = 2.2$ and the classical form for A for the energy of formation.

check nucleation rate data for scaling without assuming a value for Ω.

It is generally accepted that the discrepancies in temperature dependence arise from terms missing in the n cluster free energy of formation. And in recent years, there has been considerable progress in understanding the free energy of formation of small clusters. Several approaches have been used, including density functional theory,[33] Monte Carlo and molecular dynamics modeling of small clusters,[34−51] and modification of the classical energy of formation with small cluster size effects.[28,52,53] Underlying much recent work has been the issue of how to formulate a cluster size distribution, N_n, consistent with the statistical mechanical formulation of the dilute vapor−cluster system. One success in this area is the observation that for a supersaturated vapor consistency with the law of mass action requires that N_n be proportional to S^n. This condition is also manifest in the so-called nucleation theorem.[54,55] Many of the issues of cluster definition have been addressed for Lennard-Jones (LJ) clusters by ten Wolde and Frenkel,[56] who calculate a nucleation rate for the truncated LJ potential model.

Our interest has focused on cluster size distribution properties that might give rise to cancellation of the classical kinetic prefactor temperature dependence, $(P_o/kT)^2$, and lead to the scaling of eq 4. Classically, the n molecule cluster energy of formation has the form $An^{2/3} - n \ln S$, where $An^{2/3} = 4\pi r^2\sigma/(kT)$, and r is the classical liquid drop model cluster radius. In 1967, Fisher proposed an additional term, $\tau \ln n$,[20] which has been largely absent in the classical models for rates at $T \ll T_c$. In an attempt to see if a scaled nucleation rate might emerge from a classical "free energy difference model", we determined the n cluster energy of formation from a summation of free energy differences using the Fisher droplet model, $\Sigma_{n'=2,3,...n}\delta[An'^{2/3} + \tau \ln n' - n' \ln S]$.[27] A summation with some of the same small cluster terms was also examined by Wilemski.[52] In Figure 4 is a plot of the nucleation rate using the Fisher droplet model free energy difference summation form of the energy of formation and the classical expression for A. This approach generates additional small cluster terms for $n \leq 10$. These terms, proportional to $^2/_3An^{-1/3}$, have a different temperature dependence from the surface free energy term, $An^{*2/3} \approx {}^1/_2(2A/3 \ln S)^3 \ln S$, where n^* is the critical cluster size.

In the present work, we examine a summation technique using small cluster Helmholtz free energy differences generated with the Bennett[57] Metropolis[58] Monte Carlo technique and TIP4P[59] water−water potentials. This application of the Bennett technique is an extension of previous work on model Lennard-Jones argon clusters[36] and RSL2[60] water clusters.[37,38] The latter study of RSL2 water clusters indicated the effective surface tension of the small clusters could be approximated by a bulk value down to about $n = 10$ and that the free energy differences scale in temperature as $(T_c/T - 1)$. The RSL2 model potentials, however, produce a surface tension and a vapor pressure larger than the experimental values for water and are not useful for estimating nucleation rates. The TIP4P potentials provide an improved small cluster effective surface tension value, and the free energy differences generate an effective vapor pressure that is closer to the experimental value. The statistical mechanical formalism for n cluster concentrations, N_n, and the free energy difference calculations are described in sections II and III, respectively. In section IV the results for the nucleation rates are presented and compared to the water data. Comments and conclusions regarding the free energy difference model and its agreement with the scaled model in eq 4 are given in section V.

II. Cluster Concentrations and the Free Energy Difference Formalism

As in the previous studies,[36−38,42] it is assumed that the cluster−vapor system is a noninteracting mixture of ideal gases with each cluster size constituting an ideal gas of N_n clusters in equilibrium with N_1 monomers in a total volume, V. Further, each n cluster is described by a classical Hamiltonian with three independent configurational degrees of freedom and three independent momentum degrees of freedom per atom and an interaction potential, $U = \Sigma_{ij}U(\mathbf{r}_i - \mathbf{r}_j)$, dependent only on position vectors, $\mathbf{r}_i$. For such a system, one obtains the following expression for N_n in terms of Q_n, the canonical n cluster configurational integrals

$$\frac{N_n}{N_1{}^n} = \frac{Q_n}{n!\, Q_1{}^n} \tag{6}$$

where

$$Q_n = \int\int\int\int\cdots\int \exp\left(-\frac{\Sigma_{ij}U(\mathbf{r}_i - \mathbf{r}_j)}{kT}\right)_{n'=1,2,3..n} \prod [\mathrm{d}\mathbf{r}_{n'}/V] \tag{7}$$

The Q_n have been scaled with a V^{-n} factor and $Q_1 = 1$. After some algebra, one obtains the following expression for N_n

$$N_n = N_1 \exp\left(\sum_{n'=2,n}\left[\ln\frac{Q_{n'}}{Q_{n'-1}Q_1} - \ln\frac{n'}{N_1}\right]\right) \tag{8}$$

$$= N_1 \exp\left(\sum_{n'=2,n}[-\delta f_{n'} - I_o + \ln S_1]\right) \tag{9}$$

where

$$-\delta f_n = \ln\frac{Q_n}{Q_{n-1}Q_1(\alpha v_n/V)} + \ln\alpha \tag{10}$$

and

$$I_o \equiv \ln\frac{(n/v_n)}{(N_1^o/V)} \approx \ln\frac{\rho_{liq}}{\rho_{vap}} \tag{11}$$

The monomer supersaturation ratio is defined as $S_1 = N_1/N_1^o$, where N_1^o/V is the equilibrium number concentration of monomers. The $\alpha v_n = \alpha n/\rho_{liq}$ is the cluster simulation volume, which can be scaled with α. The goal of the present calculations is to determine the $-\delta f_n$ and generate the N_n from eq 9.

The $-\delta f_n$ in eq 9 are determined using a Bennett[57] Metropolis Monte Carlo technique[58] in which two n molecule ensembles (one an n molecule cluster and the other an $(n-1)$ molecule cluster plus free monomer) are independently simulated and constrained within a sphere of volume $\alpha v_n/V$, centered on their respective system center of mass. The $\alpha v_n/V$ factor in the denominator of eq 10 scales the $Q_1 = 1$ to $Q_1\alpha v_n/V$, introducing into the formalism the small simulation volume accessible to the monomer. Following Lee, Barker, and Abraham,[34] α is assumed to be 5. Although formally the expression in eq 9 is independent of α, the model's cluster definition becomes unrealistic if α is too large (allowing the cluster to vaporize) or too small (exerting a pressure on the constrained molecular system). For $n > 2$, the simulation results indicate effects on the order of 2% when α ranges from 5 to 7.[42] Because the center of mass transformation factors cancel in eq 10, the $-\delta f_n$ can be calculated in a fixed frame, or in the center of mass frame. The $-\delta f_n$ were calculated in both frames, and also in a center of mass frame moving all the molecules at each step. It was found that the latter technique was efficient in equilibrating the system and generating the $-\delta f_n$.

To plot and analyze the $-\delta f_n$ simulation results, the Fisher droplet model[20] form is used

$$-\delta f_n \approx I_o - \delta(A'n^{2/3} + \tau \ln n) \tag{12}$$

$$\approx I_o - \frac{2}{3}A'n^{-1/3} \quad \text{for large } n \tag{13}$$

where A' is proportional to the TIP4P effective surface tension for the small water clusters. The $I_o \approx \ln(\rho_{liq}/\rho_{vap})$ can be estimated from experiment and provides a check on the extrapolation of $-\delta f_n$ to large n. The experimental value of $\ln(\rho_{liq}/\rho_{vap}) \approx 8.9(T_c/T - 1)$ and at 280 K $I_o \approx 11.7$. Plotting $-\delta f_n$ versus $n^{-1/3}$ provides a means of examining the slope and intercept in terms of an effective surface tension and an approximate vapor pressure, both of which are dependent on the model potential. Because τ is likely to depend on n for small cluster sizes and be undetectable in $-\delta f_n$ for large cluster sizes, the τ cannot be determined from these simulations. Assuming $A' = (36\pi)^{1/3}\sigma/kT\rho_{liq}^{2/3} = (36\pi)^{1/3}\Omega(T_c/T - 1)$ as in the scaled energy of formation, one can also estimate an Ω, the excess surface entropy per molecule for the model potential. The intent in this work is to examine temperature scaling of the $-\delta f_n$ of the form $(T_c/T - 1)$ and generate simulation results useful for calculation of N_n (and nucleation rates) for a range of T.

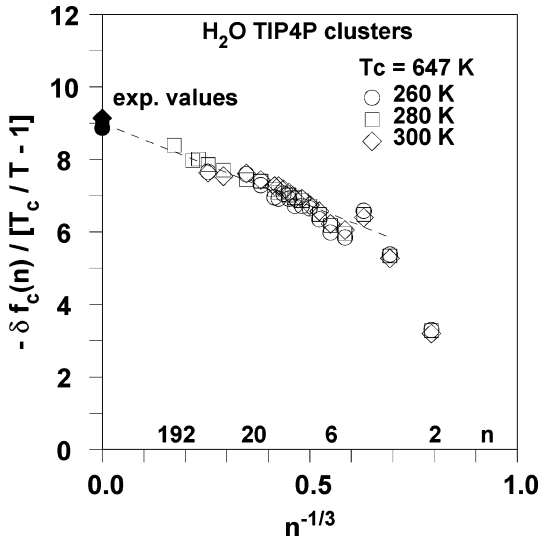

Figure 5. The calculated Monte Carlo free energy differences, $-\delta f_n/[T_c/T - 1]$, plotted versus $n^{-1/3}$ for $T = 260$ (○), 280 (□), and 300 K (◇); the intercept at $n^{-1/3} = 0$ (■) is the experimental prediction for the intercept, and the dashed line indicates the slope predicted by the experimental surface tension.

III. Small Cluster Bennett Monte Carlo Free Energy Difference Calculations

The standard Bennett technique determines the ratio of two configurational integrals over the same configuration space with differing interaction potentials. The two systems in the present case are the n system (with all of the molecules interacting normally via the TIP4P potential) and the $n-1$ plus monomer system, (with one molecule, called the probe, having its interaction with the remainder of the system reduced by a factor, λ). In these calculations, $\lambda = 10^{-7}$. The system potentials differ by $(1 - \lambda)\Delta U$, where ΔU is the interaction potential of the probe molecule. In the n system, each molecule can serve as a probe and an average over all probes is taken. Values of $-\delta f_n$ are determined after equilibration from Monte Carlo runs of length 30 to 50 million steps, using different initial configurations. The values of $-\delta f_n$ are also generated from two independently developed codes, one of which was used for binary clusters[61] and moved all of the molecules at each step.

The values of $-\delta f_n$ are calculated at $T = 260$, 280, and 300 K and plotted versus $n^{-1/3}$ in Figure 5. In this plot, the $-\delta f_n$ have been scaled by $(T_c/T - 1)$, using the experimental value, $T_c = 647$ K. Superimposed on the plot are predicted values (dashed line) using the experimental σ and ρ_{liq} to determine the slope and the experimental $\ln(\rho_{liq}/\rho_{vap})$ (filled symbols) to locate the intercept, I_o. The TIP4P free energy differences appear

to lie roughly along this line down to about $n = 6$. For clusters with less than six molecules, the $-\delta f_n$ fall off rapidly, with a characteristic peak at $n = 4$. The latter peak indicates the relative stability of the tetramer. Because of the limitations of the effective pair potential, one does not expect accurate free energy differences for $n = 2$, 3, 4, and 5. However, these calculated $-\delta f_n$ provide some measure of the effect of the smallest cluster sizes in the summation process. Uncertainties in $-\delta f_n$ are indicated by the symbol size in Figure 5. To obtain the best fit to the $-\delta f_n$, the value of T_c for the scaling was varied until the standard deviation from the average of the scaled values at each value of n was minimized. This fitting parameter, $T_{c,fit}$, was found to be 715 K. The value of $-\delta f_n$ at an arbitrary temperature can then be determined from

$$-\delta f_n(T) = \sum_{i=1,3} \frac{1}{3}\left[\frac{-\delta f_n(T_i)}{[T_{c,fit}/T_i - 1]}\right][T_{c,fit}/T - 1] \quad (14)$$

where T_i are the three temperatures, 260, 280, and 300 K. For purposes of calculating N_n and the nucleation rates, the value of $T_{c,fit}$ has no physical significance other than to generate $-\delta f_n$ at an arbitrary temperature that best fits the Monte Carlo generated free energy differences. A critical temperature of 563 $\pm$ 3 K has been reported for TIP4P.[62] However, in our analysis, it is not possible to determine T_c, and the reported value of 563 K appears to have no particular advantage in fitting or scaling the $-\delta f_n$. By use of the TIP4P Monte Carlo free energy differences, the N_n and the nucleation rates for water are calculated in the next section.

IV. Nucleation Rates for Water from Free Energy Differences

The Monte Carlo TIP4P steady-state nucleation rates, $J_{MCDS}(S,T)$, are determined from

$$\frac{1}{J_{MCDS}(S,T)} = \sum_{n=1}^{n\text{Max}} \frac{1}{J_n(S,T)} \quad (15)$$

where an efficient value of nMax can be determined by checking for independence of the sum on the upper limit value. The forward rate, $J_n(S,T)$, is given by

$$J_n(S,T) = \rho_v^o(T)\, S\, \frac{\bar{v}}{4}(36\pi)^{1/3}\left[\frac{n}{\rho_{liq}}\right]^{2/3}\frac{N_n(S,T)}{V} \quad (16)$$

where $\bar{v} = (8kT/\pi m)^{1/2}$ and

$$\frac{N_n(S,T)}{V} = \rho_v^o(T)\, S \exp \sum_{n'=2,n} [-\delta f_n - I_o(T) + \ln S] \quad (17)$$

In eq 17, the value of the equilibrium monomer concentration at temperature, T, is approximated by the experimental vapor number density, $\rho_v^o(T)$, and the monomer supersaturation ratio is approximated by the experimental S. From the Monte Carlo free energy difference calculations, it is not possible to determine the monomer concentration. In Figure 6 is shown the prediction of the nucleation rates using eqs 15−17. The values of the nucleation rates shown in Figure 6 display an improved temperature dependence and some evidence of the scaling indicated in Figure 2. However, the rates are too large by about a factor of 10^4. This was also found to be the case for TIP4P nucleation rates determined by Merikanto et al.[51] and is probably due to the value of the surface tension for TIP4P, estimated

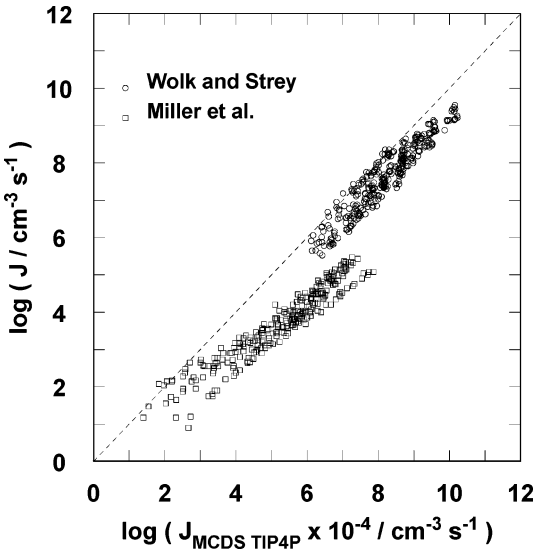

Figure 6. The experimental homogeneous nucleation rate data for water of Wölk and Strey[15] (○) and Miller et al.[7] (□) compared with the MCDS model prediction, as determined from eqs 15−17.

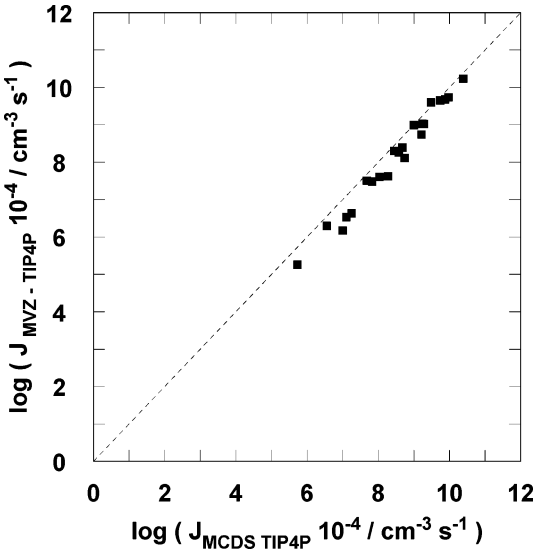

Figure 7. Comparison of the Monte Carlo TIP4P nucleation rates of Merikanto et al.,[51] J_{MVZ}, and the MCDS TIP4P nucleation rates of this work.

to be about 30% smaller than the experimental value at 298.15 K.[44,63] In Figure 7 is a comparison of the rates determined from eqs 15−17 and Merikanto et al. It is interesting that the predicted nucleation rates for the water data of Miller et al. in Figure 6 also show a marked improvement over the classical model temperature dependence and evidence of scaling.

V. Conclusions and Comments

In summary, Figures 1−4 indicate that the experimental water nucleation rates of Wölk and Strey[15] are consistent with $J_{exp} = J(\ln S/[T_c/T - 1]^{3/2})$ and the scaled nucleation model in eq 4. The Monte Carlo free energy differences for small TIP4P water clusters, when used in a discrete sum over the small cluster sizes, produce nucleation rates that appear to be partially scaled, with the largest scatter occurring at the lowest temperatures near $T = 218$ K. The other experimental rates of Wölk and Strey range from 230 to 260 K and should be better described by the simulations, the lowest temperature of which is 260 K. By making a discrete summation over $n = 2$, 3, ..., 6, one obtains

contributions to the energy of formation that have a temperature dependence different from the classical model temperature dependence. These extra terms can cancel, in part, the temperature dependence in the classical prefactor and produce nucleation rates that display temperature scaling, as observed in the experimental water data of Wölk and Strey.[15] The statistical mechanical Monte Carlo calculations of the free energy differences using TIP4P water−water potentials also scale with $(T_c/T - 1)$ at $T = 260$, 280, and 300 K, providing some insight into the origins of the scaled nucleation rate model. This scaling could be useful in computer simulations when the generation of the free energies of formation at many temperatures are required. Surprisingly, the scaling of the nucleation rates is also observed in the simple model in which one sums over small cluster free energy differences generated by the classical form for the surface free energy term. However, to obtain a correct magnitude of the nucleation rate from this approach, one must include the $\tau \ln n$ term of Fisher. It is hoped that the scaling of nucleation rates might prove useful to experimentalists and theorists and, in particular, that the scaled supersaturation will be helpful in testing experimental data for evidence of scaling.

Acknowledgment. This work was supported in part by the National Science Foundation Grant No. 93-07318. The authors thank G. Wilemski for discussions and comments and R. Strey and B. Wyslouzil for helpful comments and for generously providing their data.

References and Notes

(1) Volmer, M.; Weber A. *Z. Phys. Chem.* **1926**, *119*, 227. Volmer, M. *Kinetik der Phasenbildung*; Steinkopff: Dresden, 1939.
(2) Becker, R.; Döring, W. *Ann. Phys.* **1935**, *24*, 719.
(3) Zeldovich, Y. B. *Acta Physicochim.* **1943**, *18*, 1.
(4) Frenkel, J. *Kinetic Theory of Liquids*; Oxford University: Oxford, 1946.
(5) Abraham, F. F. *Homogeneous Nucleation Theory*; Academic Press: New York, 1974.
(6) Oxtoby, *J. Phys.: Condens. Matter* **1992**, *4*, 7627.
(7) Miller, R. C.; Anderson, R. J.; Kassner, J. L.; Hagen, D. E. *J. Chem. Phys.* **1983**, *78*, 3204.
(8) Schmitt, J. L.; Zalabsky, R. A.; Adams, G. W. *J. Chem. Phys.* **1983**, *79*, 4496.
(9) Adams, G. W.; Schmitt, J. L.; Zalabsky, R. A *J. Chem. Phys.* **1984**, *81*, 5074.
(10) Wagner, P. E.; Strey, R. *J. Chem. Phys.* **1984**, *80*, 5266.
(11) Kacker, A.; Heist, R. H. *J. Chem. Phys.* **1985**, *82*, 2734.
(12) Strey, R.; Wagner, P. E.; Schmeling, T. *J. Chem. Phys.* **1986**, *84*, 2325.
(13) Hung, C.; Krasnopoler, M. J.; Katz, J. L. *J. Chem. Phys.* **1989**, *90*, 1856.
(14) Viisanen, Y.; Strey R.; Reiss, H. *J. Chem. Phys.* **1993**, *99*, 4680.
(15) Wölk, J.; Strey, R. *J. Chem. Phys.* **2001**, *105*, 11683.
(16) Katz, J. L.; Fisk J. A.; Rudek, M. M. *Nucleation and Atmospheric Aerosols*; Kulmala, M., Wagner, P. E., Eds.; Pergamon Press: New York, 1996, p 1.
(17) Hale, B. N. *Phys. Rev. A* **1986**, *33*, 4156.
(18) Hale, B. N. *Lect. Notes Phys.* **1988**, *309*, 323.
(19) Hale, B. N. *Metallurg. Mater. Trans.* **1992**, *A23*, 1863.
(20) Fisher, M. E. *Physics* **1967**, *3*, 255.
(21) Binder, K.; Stauffer, D. *Adv. Phys.* **1976**, *25*, 343.
(22) Binder, K. *J. Phys. C* **1980**, *4*, 51. Binder, K. *Phys. Rev. A* **1982**, *25*, 1699.
(23) Hale, B. N.; Kemper, P. *J. Chem. Phys.* **1989**, *91*, 4314.
(24) Martinez, D. M.; Ferguson, F. T.; Heist, R. H.; Nuth, J. A. *J. Chem. Phys.* **2001**, *115*, 310.
(25) Wright, D.; Caldwell, R.; Moxely, C.; El-Shall, M. S. *J. Chem. Phys.* **1993**, *98*, 3356.
(26) Hale, B. N.; Kelly, B. *Chem. Phys. Lett.* **1992**, *189*, 100.
(27) Hale, B.; Han, K. In *Nucleation and Atmospheric Aerosols*; Fukuta, N., Wagner, P. E., Eds.; A. Deepak: Hampton, VA, 1992; p 133.
(28) Dillmann, A. Ph.D. Thesis, University of Göttingen, 1989. Dillmann, A.; Meier, G. E. A. *Chem. Phys. Lett.* **1989**, *160*, 71. Dillmann, A.; Meier, G. E. A. *J. Chem. Phys.* **1990**, *94*, 3872.
(29) Hale, B. N.; DiMattio, D. M. In *Nucleation and Atmospheric Aerosols 2000*; Hale, B. N., Kulmala, M., Eds.; AIP Press: Melville, NY, 2000; p 31.
(30) Wölk, J.; R. Strey, R.; Heath, C. H.; Wyslouzil, B. E. *J. Chem. Phys.* **2003**, *117*, 4954.
(31) Hale, B. To be published.
(32) Hale, B. Computer Simulations, Nucleation Rate Predictions and Scaling. In *Nucleation and Atmospheric Aerosols*; Kasahara, M., Kulmala, M., Eds.; Kyoto University Press: Kyoto, 2004; p 3.
(33) Oxtoby, D. W.; Evans, R. *J. Chem. Phys.* **1988**, *89*, 7521. Zeng, X. C.; Oxtoby, D. W. *J. Chem. Phys.* **1991**, *94*, 4472. Oxtoby, D. W. *Fundamentals of Inhomogeneous Fluids*; Henderson, D., Ed.; Marcel Dekker: New York, 1992; p 407.
(34) Lee, J. K.; Barker, J. A.; Abraham, F. F. *J. Chem. Phys.* **1973**, *58*, 3166.
(35) Wright D.; El-Shall, M. S. *J. Chem. Phys.* **1994**, *100*, 3791.
(36) Hale, B. N.; Ward, R. C. *J. Stat. Phys.* **1982**, *28*, 487.
(37) Kemper, P. A Monte Carlo Simulation of Water Clusters. Ph.D. Thesis, University of Missouri−Rolla, 1990.
(38) Hale, B. N. *Aust. J. Phys.* **1996**, *49*, 425.
(39) Akhmatskaya, E. V.; Cooper, M. D.; Burton, N. A.; Masters, A. J.; Hillier, I. H. *Chem. Phys. Lett.* **1997**, *267*, 105.
(40) Dang, L. X.; Chang, T.-M. *J. Chem. Phys.* **1997**, *106*, 8149.
(41) Kusaka, I.; Wang, Z.-G.; Seinfeld, J. H. *J. Chem. Phys.* **1998**, *108*, 3416.
(42) DiMattio, D. J. Calculation of Scaled Nucleation Rates for Water Using Monte Carlo Generated Cluster Free Energy Differences. Ph.D. Thesis, University of Missouri−Rolla, Rolla, 1999.
(43) Senger B.; Schaaf P.; Corti, S.; Bowles, R.; Pointu, D.; Voegel, J.-C.; Reiss, H. *J. Chem. Phys.* **1999**, *110*, 6438.
(44) Zakharov, V. V.; Brodskaya, E. N.; Laaksonen, A. *J. Chem. Phys.* **1997**, *107*, 10675.
(45) Schenter, G. K. *J. Chem. Phys.* **1998**, *108*, 6222.
(46) Kathmann S. M.; Schenter G. K.; Garrett, B. C. *J. Chem. Phys.* **1999**, *111*, 4688.
(47) Kusaka I.; Oxtoby, D. W. *J. Chem. Phys.* **1999**, *110*, 5249.
(48) Yasuoka, K.; Matsumoto, M. *J. Chem. Phys.* **1998**, *109*, 8463.
(49) Chen, B.; Siepmann, J. I.; Oh, K. J.; Klein, M. L. *J. Chem. Phys.* **2001**, *115*, 10903.
(50) Schenter, G. K.; Kathmann, S. M.; Garrett, B. C. *J. Chem. Phys.* **2002**, *116*, 4275.
(51) Merikanto, J.; Vehkamaki, H.; Zapadinski, *J. Chem. Phys.* **2004**, *121*, 914.
(52) Wilemski, G. *J. Chem. Phys.* **1995**, *103*, 1119.
(53) Girshick, S. L.; Chiu, C. P. *J. Chem. Phys.* **1990**, *93*, 1273.
(54) Kashchiev, D. *J. Chem. Phys.* **1982**, *76*, 5098.
(55) Oxtoby, D. W.; Kashchiev, D. *J. Chem. Phys.* **1994**, *100*, 7665.
(56) ten Wolde, P. R.; Frenkel D. *J. Chem. Phys.* **1998**, *109*, 9901. ten Wolde, P. R.; Ruiz-Montero, M. J.; Frenkel, D. *J. Chem. Phys.* **1999**, *110*, 1591.
(57) Bennett, C. H. *J. Comput. Phys.* **1976**, *22*, 245.
(58) Metropolis, M.; Rosenbluth, A.; Rosenbluth, M.; Teller, A.; Teller, E. *J. Chem. Phys.* **1953**, *121*, 087.
(59) Jorgensen, W. L.; Madura, J. D. *Mol. Phys.* **1986**, *56*, 1381.
(60) Rahman, A.; Stillinger, F. H. *J. Chem. Phys.* **1978**, *68*, 666.
(61) Kathmann, S. M.; Hale, B. N. *J. Phys. Chem. B* **2001**, *105*, 11719.
(62) Vlot, M. J.; Huinink, J.; van der Erden, J. P. *J. Chem. Phys.* **1998**, *110*, 55.
(63) Matsumoto, M.; Takaoka, Y.; Takaoka, Y. *J. Chem. Phys.* **1993**, *98*, 1464.